HHS Public Access

Author manuscript

Metabolism. Author manuscript; available in PMC 2016 June 01.

Published in final edited form as:

Metabolism. 2015 June ; 64(6): 747–755. doi:10.1016/j.metabol.2015.03.001.

Imaging human brown adipose tissue under room temperature conditions with ^{11}C-MRB, a selective norepinephrine transporter PET ligand

Janice J. Hwang[1,*], **Catherine W. Yeckel**[2,*], **Jean-Dominique Gallezot**[3], **Renata Belfort-De Aguiar**[1], **Devrim Ersahin**[3], **Hong Gao**[3], **Michael Kapinos**[3], **Nabeel Nabulsi**[3], **Yiyun Huang**[3], **David Cheng**[3], **Richard E. Carson**[3], **Robert Sherwin**[1,**], and **Yu-Shin Ding**[4,†,**]

[1]Yale University School of Medicine, Division of Endocrinology

[2]Yale School of Public Health

[3]Yale University School of Medicine, Department of Radiology, Yale PET Center

[4]New York University School of Medicine, Departments of Radiology and Psychiatry

Abstract

Introduction—Brown adipose tissue (BAT) plays a critical role in adaptive thermogenesis and is tightly regulated by the sympathetic nervous system (SNS). However, current BAT imaging modalities require cold stimulation and are often unreliable to detect BAT in the basal state, at room temperature (RT). We have shown previously that BAT can be detected in rodents under both RT and cold conditions with ^{11}C-MRB ((*S*,*S*)-^{11}C-O-methylreboxetine), a highly selective ligand for the norepinephrine transporter (NET). Here, we evaluate this novel approach for BAT detection in adult humans under RT conditions.

Methods—Ten healthy, Caucasian subjects (5 M: age 24.6±2.6, BMI 21.6±2.7 kg/m^2; 5 F: age 25.4±2.1, BMI 22.1±1.0 kg/m^2) underwent ^{11}C-MRB PET-CT imaging for cervical/supraclavicular BAT under RT and cold-stimulated conditions (RPCM Cool vest; enthalpy 15°C) compared to ^{18}F-FDG PET-CT imaging. Uptake of ^{11}C-MRB, was quantified as the distribution

†Corresponding author/requests for reprints: Yu-Shin Ding, 660 First Avenue, 4th Floor, New York, NY 10016, Phone: (212)263-6605, Fax: (212)263-7541, yu-shin.ding@nyumc.org (yushin.ding@nyu.edu).

*Contributed equally as first author to this work

**Contributed equally as senior author to this work

Author contributions

JJH and CWY contributed to study design, data collection, interpretation, and manuscript writing. JDG contributed to study design, data interpretation and manuscript editing. RBA contributed to data collection and manuscript editing. DE and DC contributed to data collection and manuscript editing. HG, MK, NN, YH contributed to study implementation. REC contributed to study design, data interpretation, and manuscript editing. RSS and YSD contributed to study idea and initiation, study design, data interpretation, and manuscript editing.

Clinical Trial Registration number: NCT 02038595

Disclosure summary: The authors report no disclosures or conflicts of interest.

volume ratio (DVR) using the occipital cortex as a low NET density reference region. Total body fat and lean body mass were assessed via bioelectrical impedance analysis.

Results—As expected, ^{18}F-FDG uptake in BAT was difficult to identify at RT but easily detected with cold stimulation (p=0.01). In contrast, BAT ^{11}C-MRB uptake (also normalized for muscle) was equally evident under both RT and cold conditions (BAT DVR: RT 1.0±0.3 vs. cold 1.1±0.3, p=0.31; BAT/muscle DVR: RT 2.3±0.7 vs. cold 2.5±0.5, p=0.61). Importantly, BAT DVR and BAT/muscle DVR of ^{11}C-MRB at RT correlated positively with core body temperature (r=0.76, p=0.05 and r=0.92, p=0.004, respectively), a relationship not observed with ^{18}F-FDG (p=0.63). Furthermore, there were gender differences in ^{11}C-MRB uptake in response to cold (p=0.03), which reflected significant differences in the change in ^{11}C-MRB as a function of both body composition and body temperature.

Conclusions—Unlike ^{18}F-FDG, the uptake of ^{11}C-MRB in BAT offers a unique opportunity to investigate the role of BAT in humans under basal, room temperature conditions.

Keywords

human brown adipose tissue; norepinephrine transporter; ^{11}C-MRB; (*S,S*)-^{11}C-O-methylreboxetine; positron emission tomography (PET); sympathetic nervous system

1. INTRODUCTION

Brown adipose tissue (BAT) has reemerged over the last decade as a potential target for modulating human energy homeostasis. Although early histological evidence supported the presence of BAT in humans throughout all stages of life [1], BAT was, until recently, believed to have minimal biological impact in adult humans. With the advent of imaging modalities such as positron emission tomography coupled with CT (PET-CT) and selective tissue sampling to confirm the presence BAT, there is now undisputed evidence that functional BAT does exist into adulthood [1-3]. Furthermore, BAT likely plays a significant role in energy homeostasis and thermogenesis [2, 4]. However, current methodology to measure BAT has revealed limitations in our ability to assess the true magnitude of BAT's role in energy homeostasis because most available methods to detect BAT require activation of BAT and are unreliable in assessing BAT under basal conditions despite evidence that BAT is tonically active and consumes oxygen on average 300% higher than subcutaneous white adipose tissue under basal conditions [5]. Thus, understanding the role of BAT in humans under normal daily conditions will be critical in determining its efficacy as a target for the treatment of diabetes and obesity.

Most recent studies investigating the potential of BAT in adaptive thermogenesis have focused on assessing the effects of BAT following activation (either using cold stimulation or pharmacotherapy) as a potential therapy for diabetes or obesity. Although these studies show that following acute activation, BAT may provide a means to improve glucose control [6, 7] as well as shift the total energy balance [8, 9] to favor weight loss, the extent to which BAT contributes to energy expenditure is unclear for humans. Studies estimating the potential impact of BAT in humans have estimated that BAT could contribute between 2-5% of basal metabolic rate [3, 9, 10]; however, these modest effects were calculated from estimates of quantity of cold-activated BAT, and there have been no standard methods to

reliably quantify BAT tissue in humans. Most importantly, these studies did not address the impact of basal BAT on human energy homeostasis despite strong evidence that BAT is tonically active [5, 11-13].

One reason that less attention has been focused on basal BAT is because the standard imaging modality for BAT, ^{18}F-2-fluoro-deoxy-D-glucose (^{18}F-FDG) PET-CT, largely requires cold stimulation in order to visualize BAT. While ^{18}F-FDG is well-established for the study of acute BAT activation, it is unreliable when used to study human BAT in the room temperature, basal state. Studies using ^{18}F-FDG to measure BAT under room-temperature conditions have reported a prevalence of detectable BAT in less than 10% of subjects [14]. In one study of 17 subjects, histologically confirmed BAT was detected in all subjects; however,^{18}F-FDG PET-CT scanning positively detected BAT in only 3 of these subjects [15]. In another study, 33 subjects had 5 repeated ^{18}F-FDG scans and only 1 subject had reproducibly detectable BAT on all 5 scans at ambient conditions [16]. Even following cold stimulation, prevalence of BAT detected using ^{18}F-FDG has been variable with rates ranging from 30-100% in adults [4, 17, 18]. These variable findings reflect our lack of understanding of all the factors that regulate BAT and also underscore the fact that ^{18}F-FDG is only tracing one property of BAT, namely glucose uptake in BAT despite the fact that free fatty acids are the primary substrate for BAT [19]; thus, alternative and complimentary imaging modalities to ^{18}F-FDG imaging are needed in order to comprehensively investigate the role of human BAT in its basal state as well as following acute activation.

Basal tone in BAT is tightly regulated by the sympathetic nervous system, beginning in the central thermoregulatory centers of the hypothalamus and extending to a dense network of postganglionic neurons [20]. Sympathetic tone has been shown to modulate many aspects of BAT physiology beyond its acute activation, including brown adipocyte differentiation, recruitment, and efficacy of BAT for thermogenesis [11-13]. In cell culture experiments with brown preadipocytes, norepinephrine promotes proliferation [11], furthermore, constant norepinephrine stimulation increases the amount of mitochondria in the brown adipocytes which increases their oxidative capacity [12]. Finally, basal SNS tone has been shown in rats to be necessary in order to achieve maximal stimulation of BAT [13].

SNS activity in BAT is mediated principally by the neurotransmitter, norepinephrine and relies on recycling of norepinephrine by the norepinephrine transporter (NET), which is present on all adrenergic neurons and is responsible for re-uptake and re-packaging of 80-90% of synaptic norepinephrine [21]. Because of the critical importance of the sympathetic nervous system in both basal and activated BAT, we sought to non-invasively measure BAT SNS innervation by using ^{11}C-MRB ((*S*,*S*)-^{11}C-O-methylreboxetine), a highly selective ligand for the NET which has been well characterized in human and non-human primate CNS studies [22-26]. We hypothesized that ^{11}C-MRB would be a novel and specific label for the degree of sympathetic innervation of BAT which would allow a unique assessment of BAT in its basal state. Our initial studies in a rodent model identified that NET could be a highly specific target for BAT [27], and we have shown that BAT can be detected in rodents under both room temperature and cold conditions. Furthermore, the uptake of ^{11}C-MRB in BAT was completely abolished by the pretreatment with a NET inhibitor, demonstrating the ligand specific labeling of BAT [27]. In this study, we

compare ^{11}C-MRB and ^{18}F-FDG uptake in BAT through PET-CT scanning to address whether ^{11}C-MRB can be used as a novel means of imaging basal BAT in humans under room temperature conditions. Furthermore, we take advantage of this mechanistically-driven BAT ligand to examine the relationships between gender and body temperature and body composition parameters on basal BAT.

2. MATERIALS AND METHODS

2.1. Participants

Young, healthy Caucasian participants were recruited through public advertisements in the greater New Haven area (Table 1). Exclusion criteria included any medical problems including diabetes mellitus; thyroid, cardiovascular, pulmonary disease; smoking and illicit drug use; use of any medications with the exception of hormonal contraception for women. The one female participant who was not receiving hormonal contraception underwent all scanning during the luteal phase of menstrual cycle. Subjects refrained from any grapefruit products, excessive physical activity beyond their normal routine or alcohol use for 3 days prior to and after each scan. The protocol (ClinTrials NCT 02038595) was approved by the Yale University Human Investigation and Radiation Safety Committees.

All subjects provided informed, written consent before participation in the study. Each subject underwent a physical exam, electrocardiogram, blood testing, and a urine toxicology screen. Baseline anthropometric measurements were obtained including height, weight and total body fat measured by bioelectrical impedance analysis (Tanita body composition analyzer, model TBF-300)).

2.2 Study Design

Subjects underwent PET-CT imaging using ^{11}C-MRB as well as ^{18}F-FDG under room temperature (RT) and mild cold stimulated conditions (RPCM Cool vest, Glacier Tek, Inc, USA; enthalpy rated at 15°C). Given the minimal information obtained from RT ^{18}F-FDG scans based on our initial data, and in an effort to minimize radiation exposure for female subjects, a subset of 3 women did not undergo ^{18}F-FDG PET-CT imaging at RT. Cold condition scans were performed while subjects wore a climate vest loaded with cold packs, whereas room temperature scans were conducted using the same climate vest loaded with RT packs, to avoid potential biases from changes in attenuation between the two conditions.

For ^{18}F-FDG studies, subjects wore the climate vest for half an hour before ^{18}F-FDG injection, during the 60-minute period between the injection, and during the 25-30 minute scan. For ^{11}C-MRB PET-CT scans, the climate vest was placed on the subjects 30 min prior to intravenous ^{11}C-MRB administration and remained on the subject for the duration of the 120-125 minute dynamic scan. PET-CT scanning began with the administration of ^{11}C-MRB.

All scans were performed under fasting conditions. Studies performed at RT were always conducted in the morning and cold stimulated conditions were performed in the afternoon. This was necessary to avoid the potential physiological carryover of a prior cold condition in the case of two scans being carried out on the same day. ^{18}F-FDG and ^{11}C-MRB scans were

separated by at least 1 week and all subjects completed all scans within 4 weeks. Shivering was neither reported by study participants nor observed by research staff.

Vitals signs including tympanic body temperature (Braun PRO 4000, USA), blood pressure and heart rate were obtained during each scan immediately prior to and 30 minutes after wearing the vest. Body temperature at RT was missing for 1 male subject.

2.3. PET-CT Protocols

^{11}C-MRB was synthesized at the Yale PET center based on procedures described previously [28]. The specific activity at the end of synthesis was 639 ± 319 MBq/nmol and the radiochemical purity was ≥ 99.4%. ^{18}F-FDG was purchased from IBA Molecular (USA).

PET imaging was performed using the mCT PET/CT scanner (Siemens/CTI, USA). Subjects were in supine position with arms at their side. Five to six bed positions were used to scan from the head to the lower abdomen. Before each PET scan, a CT scan (2 mm slice thickness) was performed with the same number of bed positions for attenuation correction and to help delineate the BAT region of interest.

For ^{18}F-FDG scans, one cycle through all bed positions was performed, with a 5-min acquisition for each bed position. For ^{11}C-MRB scans, 13 (12, respectively) cycles through all 5 (6, respectively) bed positions were performed, with the following per bed acquisition times: 18 seconds for 2 cycles, 36 seconds for 3 cycles, 72 seconds for 3 cycles, 180 seconds for 3 cycles, 300 seconds for 2 (1, respectively) cycle(s). Images were reconstructed with an OSEM algorithm using point spread function and time-of-flight corrections. Images from different bed positions were combined to provide a whole body image with 363 (for 5 bed positions) or 425-426 (for 6 bed positions) transverse slices.

2.4. Co-registration

To correct for body motion during the ^{11}C-MRB scans, each frame of the dynamic scan was co-registered to a reference sum image using a 12-parameter affine transforms followed by a nonlinear transformation grid. The transforms were estimated using the Bioimagesuite software (version 2.5; http://www.bioimagesuite.com) [29].

To co-register the two ^{11}C-MRB scans and the two ^{18}F-FDG scans together, a sum image (0 to 120 min) was computed for each of the ^{11}C-MRB scans, then the cold condition ^{11}C-MRB sum image and the two ^{18}F-FDG static images were co-registered to the baseline ^{11}C-MRB sum image using a 12-parameter affine transforms followed by a nonlinear transformation, using the same software as for the motion correction of ^{11}C-MRB scans.

2.5. Regions of Interest

Supraclavicular and cervical BAT ROIs were manually delineated by an American Board of Nuclear Medicine certified physician on cold ^{18}F-FDG static images. CT images were visually examined to ensure that the attenuation coefficient corresponded to fat tissue using a HU window (-50 to -200 HU) to enhance contrast between fat and other non-fat soft tissue. Muscle ROIs were drawn on CT images in the deltoid muscle. Brain region of interest for the occipital cortex was taken from an MR template [30], which was co-registered with

the ^{11}C-MRB scans using an early sum image (0-10 min post injection) and an affine (12 parameters) transforms.

2.6. Analysis

For analysis of tracer uptake, mean SUV, rather than max SUV used for tumors, is reported given the relative homogeneity of the adipose tissue. SUV images were also used for visualization. Given the lack of standardized definitions of BAT, we chose an ^{18}F-FDG SUV >1.5 and Hounsfield units (-200 to -50) as has been used by others [7, 31] to define BAT tissue. In contrast to ^{18}F-FDG, ^{11}C-MRB is a reversible, competitive tracer. Because the distribution volume ratio (DVR) is a more precise measurement of uptake for reversible tracers [32] such as ^{11}C-MRB, we quantified regional ^{11}C-MRB uptake as DVR, estimated via MRTM2 [25, 33] (t*=30 min) using the occipital cortex, a region with low NET density [25, 34], as the reference region. MRTM2 reduces the variability of MRTM [33] parameter estimates by fixing one of the three parameters, the parameter k2', which is only related to the reference region time-activity curve, to a common value for all regions/voxels. In this study, the parameter k2' was fixed to 0.021 min^{-1}, based on previous brain studies. Furthermore, the tracer binding has been well-characterized in our previous brain studies in humans [22, 25, 26, 35] and uptake of metabolites of ^{11}C-MRB was minimal in rodent BAT [27]. Muscle was also chosen as a peripheral reference, and a ratio of BAT-DVR to muscle-DVR (BAT/muscle) was compared.

2.7. Statistical Analysis

Two-sided paired sample t-tests were used to compare ^{18}F-FDG and ^{11}C-MRB scans under room temperature and cold stimulated conditions. Two-sided independent sample t-tests were used assess gender differences. Correlations between variables were determined with a Pearson correlation coefficient. Data analysis was performed using SPSS software (version 21.0, IBM). *P* values of less than 0.05 were considered statistically significant.

3. RESULTS

3.1 Subject Characteristics

As shown in Table 1, there were no differences in age or body mass index (BMI) between men and women. Compared to men, women had significantly higher fat mass and lower lean mass as measured by bioelectric impedance. There were no differences in baseline body temperature, resting heart rate, or systolic blood pressure between men and women. Men had slightly higher baseline diastolic blood pressure and mean arterial pressures compared to women.

3.2 ^{11}C-MRB and ^{18}F-FDG BAT Labeling

Eight out of ten subjects had BAT detected on all three scans (cold ^{18}F-FDG, RT ^{11}C-MRB and cold ^{11}C-MRB) (Figure 1). Furthermore, the ^{11}C-MRB quantitative measures at RT and cold conditions were comparable (DVR: RT 1.0 ± 0.3 vs. cold 1.1 ± 0.3, $p = 0.31$; DVR (BAT/muscle): RT 2.3 ± 0.7 vs. cold 2.5 ± 0.5, $p = 0.61$; Figure 2). In contrast, BAT was difficult to identify for ^{18}F-FDG at RT with significantly lower SUV at RT than with cold stimulation (RT 0.8 ± 0.3 vs. cold 3.2 ± 1.5, $p = 0.01$). The 2 subjects that did not have BAT

detected on all three scans were female. One subject had no visibly detected BAT on any scans. The other subject had no BAT detected on the cold ^{18}F-FDG scan; however, BAT was both visually and quantitatively detected on the ^{11}C-MRB cold and RT scans (DVR 1.1 and 1.6, respectively) and in similar values to group means. There were no differences in body composition or physical exam between these two subjects and other subjects.

Overall, there were no differences in ^{18}F-FDG uptake during the cold scan between men and women (men 3.4 ± 1.6 vs. women 2.9 ± 1.7, $p = 0.7$) or in ^{11}C-MRB uptake both during the RT (men 0.9 ± 0.2 vs. women 1.1 ± 0.4, $p = 0.7$) and cold scans (men 1.2 ± 0.3 vs. women 0.9 ± 0.2, $p = 0.3$) (Figure 2).

The relative ability of ^{18}F-FDG and ^{11}C-MRB to detect BAT located in additional, previously described depots throughout the body [1] was compared under both RT and cold conditions. Two ABNM certified physicians independently inspected the scans of all subjects for presence of BAT in the axillary, paraspinal, mediastinal, and suprarenal regions. For the paraspinal and mediastinal regions, visual inspection noted minimal ^{18}F-FDG uptake at RT; however, cold ^{18}F-FDG as well as RT and cold ^{11}C-MRB scans detected BAT with similar frequencies. There was variability between the physicians in the ability to reliably distinguish BAT from nearby tissues particularly in the suprarenal, and to a lesser extent axillary, regions for both FDG and MRB scans.

3.3. ^{11}C-MRB Uptake, Body Temperature, and Body Composition

Under fasting, morning, RT conditions, there was a positive correlation between baseline body temperature and baseline ^{11}C-MRB uptake in BAT, which remained significant after normalization to muscle (BAT DVR: $r = 0.76$, $p = 0.05$; BAT/muscle DVR ratio $r = 0.92$, $p = 0.004$) (Figure 3A and B). This relationship was not observed with^{18}F-FDG scanning.

There were no significant correlations between body temperature after cold stimulation with either ^{11}C-MRB ($p = 0.39$) or ^{18}F-FDG uptake ($p = 0.63$) after cold. However, the change in MRB uptake in response to cold (Figure 4) negatively correlated with body temperature after 30 minutes of cold exposure ($r = -0.74$, $p = 0.01$). This correlation was driven by differences between men and women, with men having significantly increased ^{11}C-MRB uptake in response to cold ($p = 0.03$) and lower body temperatures compared to women who tended to have decreased MRB uptake in response to cold and also higher body temperatures after 30 minutes of cold exposure (Figure 4A and 4B). Furthermore, in a similar pattern, men also tended to have higher baseline mean arterial blood pressures which correlated positively with increased ^{11}C-MRB uptake in response to cold ($r = 0.81$, $p = 0.02$). There were no relationships between ^{11}C-MRB uptake and heart rate or BMI. However, the magnitude of change in ^{11}C-MRB BAT uptake in response to cold correlated negatively with percent body fat ($r = -0.74$, $p = 0.04$) and positively with lean mass ($r = 0.71$, $p = 0.05$) (Figure 4C and D), which also showed a gender difference. There were no relationships between the change in ^{18}F-FDG uptake in response to cold and body composition, BMI, body temperature, heart rate or blood pressure.

4. DISCUSSION

By targeting the NET element of the sympathetic nervous system innervation of BAT, we provide the first evidence that ^{11}C-MRB PET-CT imaging can label human BAT. This imaging modality, therefore, offers an alternative and complimentary approach to the standard ^{18}F-FDG imaging which has been well validated to assess BAT following cold stimulation, but is unreliable when assessing basal BAT. Importantly, in this proof of concept study, we show that ^{11}C-MRB is effective in labeling BAT under basal conditions and thus may provide an assessment of the individual's tonically active BAT tissue.

Our findings in humans are consistent with our preclinical rodent studies showing intense ^{11}C-MRB uptake in interscapular BAT detected under both room temperature and cold-exposed rats; in contrast, ^{18}F-FDG in BAT was only detected in rats following cold stimulation [27]. Furthermore, even with cold stimulation there was not a dramatic increase in ^{11}C-MRB uptake. This finding suggests that unlike other NE analogs [36, 37] which measure acute sympathetic activity, ^{11}C-MRB, which targets the NET, has the potential to serve as a tracer for an intrinsic component of the SNS innervation of BAT. By targeting the SNS innervation of BAT tissue rather than the acute activation of BAT, we observed a positive relationship between basal body temperature and ^{11}C-MRB uptake in BAT. Although interpretation of our data may be tempered by the small sample size, this preliminary evidence suggests that the degree of sympathetic innervation of BAT may play a significant role in the set-point for basal body temperature. Furthermore, these data provide evidence that basal BAT activity plays a role in helping to support energy expenditure during the resting state; e.g., room temperature.

In this study, one subject did not have any BAT detected on any scans. The true prevalence of BAT in the human population remains uncertain; however, our findings are consistent with reports in the literature. Lee et al have reported that roughly 5% of individuals (1 out of 17) did not have histological evidence of BAT tissue obtained from supraclavicular biopsy [15]. In an autopsy study, Heaton showed that roughly 20% of subjects aged 20-30 years did not have BAT detected in the clavicular region [1]. However, BAT was present in many other depots in the body and decreased with age. These studies highlight the fact that many variables may play into the regulation of BAT in the human body. Furthermore, one female subject did not have any BAT identified on cold ^{18}F-FDG scanning, but had BAT detected both visually and quantitatively on the ^{11}C-MRB cold and RT scans in values similar to group means. One explanation for this is that ^{18}F-FDG imaging, by assessing the degree of glucose consumption in BAT, may not reflect other factors that regulate BAT metabolic activity particularly because the primary substrate for BAT is free fatty acids [38]. Notably, when we included this subject in the analysis, the correlations we report persisted (^{11}C-MRB BAT at RT correlated positively with body temp at RT (r = 0.78, p = 0.02) and ^{11}C-MRB BAT uptake in response to cold correlated negatively with percent body fat (r = -0.68, p = 0.04) and positively with lean mass (r = 0.80, p = 0.01)).

While reports in the literature have been conflicted regarding gender differences in BAT with evidence both for [2] and against any differences [39, 40], we observed that using ^{11}C-MRB, men and women in our study had different patterns of response to cold stimulation.

Compared to men, the women exhibited a smaller increase in ^{11}C-MRB uptake in response to cold, which correlated with their higher body temperatures. Mechanistically, this smaller increase in uptake corresponds to greater local NE release to compete with the ^{11}C-MRB NET binding and thus is interpreted as increased sympathetic stimulation. Importantly, although men and women had similar BMIs, they had very different lean body mass and percent body fat compositions, and thus more studies will be needed to delineate the specific factors influencing our findings, particularly whether these gender differences are driven simply by body composition, actual BAT mass, or in the varying factors that contribute to the total thermogenic potential of the BAT tissue.

To indirectly explore these factors influencing BAT, we capitalized on the fact that blood flow in BAT increases in response to cold stimulation [10, 41] and that, in rodents, immunohistochemical localization of NET in BAT is notable for dense staining of NET along capillary blood vessels and only mild staining along the plasma membrane of BAT cells themselves [42]. One advantage of using ^{11}C-MRB may be the ability to calculate perfusion based on tracer kinetics. We estimate that blood flow at baseline was lower in men than women (data not shown). Although blood flow tended to increase in response to cold, blood flow in men never exceeded the blood flow in the women during cold stimulation. While our study was not designed to assess perfusion in BAT, this picture is consistent with data showing that men had less BAT activation overall in association with a lower body temperature after cold exposure.

Whether the presence and/or activity of BAT is altered by obesity remains uncertain. We saw no relationship between ^{11}C-MRB uptake in BAT and BMI although our findings may have been limited by the small sample size and the fact that all of our subjects were normal weight. While there have been studies reporting lower prevalence of detectable BAT with increasing BMI and body fat [2, 4, 43, 44], it remains unclear whether these observations are driven by changes in cold-sensing seen in obesity [45] or a true decrease in BAT mass. ^{18}F-FDG studies reporting BAT is diminished in obesity [2, 4, 43, 44] may be limited by the fact that obese individuals have greater insulation and capacity to retain heat than lean individuals, thereby requiring greater cold stimulation to activate a BAT thermogenic response. Interestingly, obesity has been associated with decreased NET availability in brain regions important in energy homeostasis and temperature regulation [22]. ^{11}C-MRB has been well validated for use in studying NET in the human brain [22, 25, 26, 35] because it readily crosses the blood-brain barrier. Given the clear evidence that BAT is under central SNS regulation, ^{11}C-MRB has the potential to facilitate simultaneous assessment of the SNS activity both centrally and peripherally, e.g., in BAT.

Our proof of concept study does have some limitations including a small sample size and the relatively homogeneous subject population, which was young, relatively lean, and Caucasian. Additional studies will be needed to determine whether individuals of varying body mass, ethnicity, gender, or age will have different patterns of SNS innervation of BAT as assessed by ^{11}C -MRB imaging. Also, we chose to compare the current standard imaging modality for BAT, ^{18}F-FDG PET-CT scanning following cold stimulation, to ^{11}C-MRB imaging rather than the more invasive, gold standard biopsy confirmation of BAT. Notably, in rodent studies comparing the % injected dose (ID) of ^{11}C-MRB and ^{18}F-FDG normalized

to grams of BAT tissue, we have shown previously that the %ID of ^{18} F-FDG was significantly less than the %ID of ^{11}C-MRB under RT conditions [27]. Because ^{18}F-FDG labeling is dependent on the glucose consumption rate of BAT, it has proven to be a less reliable label for BAT under RT conditions. MRB, in contrast, labels the degree of sympathetic innervation of BAT, which as seen in our figures, is independent of ambient temperature related stimuli and thus may allow for a more reliable labeling of BAT under tonic RT conditions.

With the growing clinical interest in harnessing the thermogenic properties of BAT for treatment of diabetes and obesity, understanding the mechanisms behind how BAT interplays with these metabolic diseases requires assessment of not only factors that activate existing BAT, but also the factors that regulate how much BAT is present in the body and how effective the BAT tissue is at thermogenesis. Thus, a complete determination of the thermogenic potential of human BAT requires not only assessment of BAT following acute stimulation, but also BAT in its basal state. Here, we show that ^{11}C-MRB can be used to detect basal human BAT without cold stimulation. By directly assessing the degree of tonic sympathetic activity of BAT, this methodology offers unique advantages for further investigation into the factors beyond cold stimulation that may play an important role in the regulation of human BAT.

Acknowledgments

The authors gratefully acknowledge the participants of the study as well as the nurses and staff at the Yale University PET Center.

Grant support: This publication was made possible by DK09076 as well as CTSA Grant Number UL1 TR000142 from the National Center for Advancing Translational Science (NCATS), a component of the National Institutes of Health (NIH). Its contents are solely the responsibility of the authors and do not necessarily represent the official view of NIH.

References

1. Heaton JM. The distribution of brown adipose tissue in the human. J Anat. 1972; 112(Pt 1):35–9. [PubMed: 5086212]
2. Cypess AM, Lehman S, Williams G, Tal I, Rodman D, Goldfine AB, et al. Identification and importance of brown adipose tissue in adult humans. N Engl J Med. 2009; 360(15):1509–17. [PubMed: 19357406]
3. Virtanen KA, Lidell ME, Orava J, Heglind M, Westergren R, Niemi T, et al. Functional brown adipose tissue in healthy adults. N Engl J Med. 2009; 360(15):1518–25. [PubMed: 19357407]
4. Saito M, Okamatsu-Ogura Y, Matsushita M, Watanabe K, Yoneshiro T, Nio-Kobayashi J, et al. High incidence of metabolically active brown adipose tissue in healthy adult humans: effects of cold exposure and adiposity. Diabetes. 2009; 58(7):1526–31. [PubMed: 19401428]
5. Vijgen GH, Sparks LM, Bouvy ND, Schaart G, Hoeks J, van Marken Lichtenbelt WD, et al. Increased oxygen consumption in human adipose tissue from the “brown adipose tissue” region. J Clin Endocrinol Metab. 2013; 98(7):E1230–4. [PubMed: 23783102]
6. Chondronikola M, Volpi E, Borsheim E, Porter C, Annamalai P, Enerback S, et al. Brown adipose tissue improves whole-body glucose homeostasis and insulin sensitivity in humans. Diabetes. 2014; 63(12):4089–99. [PubMed: 25056438]
7. Lee P, Smith S, Linderman J, Courville AB, Brychta RJ, Dieckmann W, et al. Temperature-acclimated brown adipose tissue modulates insulin sensitivity in humans. Diabetes. 2014; 63(11): 3686–98. [PubMed: 24954193]

8. Rothwell NJ, Stock MJ. Diet-induced thermogenesis. Adv Nutr Res. 1983; 5:201–20. [PubMed: 6342342]
9. van Marken Lichtenbelt WD, Schrauwen P. Implications of nonshivering thermogenesis for energy balance regulation in humans. Am J Physiol Regul Integr Comp Physiol. 2011; 301(2):R285–96. [PubMed: 21490370]
10. Muzik O, Mangner TJ, Leonard WR, Kumar A, Janisse J, Granneman JG. 15O PET measurement of blood flow and oxygen consumption in cold-activated human brown fat. J Nucl Med. 2013; 54(4):523–31. [PubMed: 23362317]
11. Bronnikov G, Bengtsson T, Kramarova L, Golozoubova V, Cannon B, Nedergaard J. beta1 to beta3 switch in control of cyclic adenosine monophosphate during brown adipocyte development explains distinct beta-adrenoceptor subtype mediation of proliferation and differentiation. Endocrinology. 1999; 140(9):4185–97. [PubMed: 10465291]
12. Nechad M, Nedergaard J, Cannon B. Noradrenergic stimulation of mitochondriogenesis in brown adipocytes differentiating in culture. Am J Physiol. 1987; 253(6 Pt 1):C889–94. [PubMed: 2827500]
13. Festuccia WT, Blanchard PG, Richard D, Deshaies Y. Basal adrenergic tone is required for maximal stimulation of rat brown adipose tissue UCP1 expression by chronic PPAR-gamma activation. Am J Physiol Regul Integr Comp Physiol. 2010; 299(1):R159–67. [PubMed: 20393157]
14. Lee P, Swarbrick MM, Ho KK. Brown adipose tissue in adult humans: a metabolic renaissance. Endocr Rev. 2013; 34(3):413–38. [PubMed: 23550082]
15. Lee P, Zhao JT, Swarbrick MM, Gracie G, Bova R, Greenfield JR, et al. High prevalence of brown adipose tissue in adult humans. J Clin Endocrinol Metab. 2011; 96(8):2450–5. [PubMed: 21613352]
16. Rousseau C, Bourbouloux E, Campion L, Fleury N, Bridji B, Chatal JF, et al. Brown fat in breast cancer patients: analysis of serial (18)F-FDG PET/CT scans. Eur J Nucl Med Mol Imaging. 2006; 33(7):785–91. [PubMed: 16596378]
17. Yoneshiro T, Aita S, Matsushita M, Okamatsu-Ogura Y, Kameya T, Kawai Y, et al. Age-related decrease in cold-activated brown adipose tissue and accumulation of body fat in healthy humans. Obesity (Silver Spring). 2011; 19(9):1755–60. [PubMed: 21566561]
18. Orava J, Nuutila P, Lidell ME, Oikonen V, Noponen T, Viljanen T, et al. Different metabolic responses of human brown adipose tissue to activation by cold and insulin. Cell Metab. 2011; 14(2):272–9. [PubMed: 21803297]
19. Ma SW, Foster DO. Uptake of glucose and release of fatty acids and glycerol by rat brown adipose tissue in vivo. Can J Physiol Pharmacol. 1986; 64(5):609–14. [PubMed: 3730946]
20. Cerri M, Morrison SF. Activation of lateral hypothalamic neurons stimulates brown adipose tissue thermogenesis. Neuroscience. 2005; 135(2):627–38. [PubMed: 16125857]
21. Boschmann M, Schroeder C, Christensen NJ, Tank J, Krupp G, Biaggioni I, et al. Norepinephrine transporter function and autonomic control of metabolism. J Clin Endocrinol Metab. 2002; 87(11): 5130–7. [PubMed: 12414883]
22. Li CS, Potenza MN, Lee DE, Planeta B, Gallezot JD, Labaree D, et al. Decreased norepinephrine transporter availability in obesity: Positron Emission Tomography imaging with (S,S)-[(11)C] O-methylreboxetine. Neuroimage. 2014; 86:306–10. [PubMed: 24121204]
23. Ding YS, Lin KS, Logan J, Benveniste H, Carter P. Comparative evaluation of positron emission tomography radiotracers for imaging the norepinephrine transporter: (S,S) and (R,R) enantiomers of reboxetine analogs ([11C]methylreboxetine, 3-Cl-[11C]methylreboxetine and [18F]fluororeboxetine), (R)-[11C]nisoxetine, [11C]oxaprotiline and [11C]lortalamine. J Neurochem. 2005; 94(2):337–51. [PubMed: 15998285]
24. Gallezot JD, Weinzimmer D, Nabulsi N, Lin SF, Fowles K, Sandiego C, et al. Evaluation of [(11)C]MRB for assessment of occupancy of norepinephrine transporters: Studies with atomoxetine in non-human primates. Neuroimage. 2011; 56(1):268–79. [PubMed: 20869448]
25. Hannestad J, Gallezot JD, Planeta-Wilson B, Lin SF, Williams WA, van Dyck CH, et al. Clinically relevant doses of methylphenidate significantly occupy norepinephrine transporters in humans in vivo. Biol Psychiatry. 2010; 68(9):854–60. [PubMed: 20691429]

26. Ding YS, Singhal T, Planeta-Wilson B, Gallezot JD, Nabulsi N, Labaree D, et al. PET imaging of the effects of age and cocaine on the norepinephrine transporter in the human brain using (S,S)-[(11)C]O-methylreboxetine and HRRT. Synapse. 2010; 64(1):30–8. [PubMed: 19728366]
27. Lin SF, Fan X, Yeckel CW, Weinzimmer D, Mulnix T, Gallezot JD, et al. Ex vivo and in vivo evaluation of the norepinephrine transporter ligand [11C]MRB for brown adipose tissue imaging. Nucl Med Biol. 2012; 39(7):1081–6. [PubMed: 22595487]
28. Lin KS, Ding YS. Synthesis, enantiomeric resolution, and selective C-11 methylation of a highly selective radioligand for imaging the norepinephrine transporter with positron emission tomography. Chirality. 2004; 16(7):475–81. [PubMed: 15236345]
29. Papademetris X, Jackowski AP, Schultz RT, Staib LH, Duncan JS. Integrated Intensity and Point-Feature Nonrigid Registration. Med Image Comput Comput Assist Interv. 2001; 3216(2004):763–70. [PubMed: 20473359]
30. Tzourio-Mazoyer N, Landeau B, Papathanassiou D, Crivello F, Etard O, Delcroix N, et al. Automated Anatomical Labeling of Activations in SPM Using a Macroscopic Anatomical Parcellation of the MNI MRI Single-Subject Brain. Neuroimage. 2002; 15(1):273–89. [PubMed: 11771995]
31. Blondin DP, Labbe SM, Tingelstad HC, Noll C, Kunach M, Phoenix S, et al. Increased brown adipose tissue oxidative capacity in cold-acclimated humans. J Clin Endocrinol Metab. 2014; 99(3):E438–46. [PubMed: 24423363]
32. Innis RB, Cunningham VJ, Delforge J, Fujita M, Gjedde A, Gunn RN, et al. Consensus nomenclature for in vivo imaging of reversibly binding radioligands. Journal of Cerebral blood flow and metabolism. 2007; 27(9):1533–9. [PubMed: 17519979]
33. Ichise M, Liow J-S, Lu J-Q, Takano A, Model K, Toyama H, et al. Linearized reference tissue parametric imaging methods: application to [11C]DASB positron emission tomography studies of the serotonin transporter in human brain. Journal of Cerebral blood flow and metabolism. 2003; 23(9):1096–112. [PubMed: 12973026]
34. Schou M, Halldin C, Pike VW, Mozley PD, Dobson D, Innis RB, et al. Post-mortem human brain autoradiography of the norepinephrine transporter using (S,S)-[18F]FMeNER-D2. Eur Neuropsychopharmacol. 2005; 15(5):517–20. [PubMed: 16139169]
35. Pietrzak RH, Gallezot JD, Ding YS, Henry S, Potenza MN, Southwick SM, et al. Association of posttraumatic stress disorder with reduced in vivo norepinephrine transporter availability in the locus coeruleus. JAMA Psychiatry. 2013; 70(11):1199–205. [PubMed: 24048210]
36. Thackeray JT, Beanlands RS, Dasilva JN. Presence of specific 11C-meta-Hydroxyephedrine retention in heart, lung, pancreas, and brown adipose tissue. J Nucl Med. 2007; 48(10):1733–40. [PubMed: 17873125]
37. Admiraal WM, Holleman F, Bahler L, Soeters MR, Hoekstra JB, Verberne HJ. Combining 123I-metaiodobenzylguanidine SPECT/CT and 18F-FDG PET/CT for the assessment of brown adipose tissue activity in humans during cold exposure. J Nucl Med. 2013; 54(2):208–12. [PubMed: 23318291]
38. Enerback S. Human brown adipose tissue. Cell Metab. 2010; 11(4):248–52. [PubMed: 20374955]
39. van der Lans AA, Hoeks J, Brans B, Vijgen GH, Visser MG, Vosselman MJ, et al. Cold acclimation recruits human brown fat and increases nonshivering thermogenesis. J Clin Invest. 2013; 123(8):3395–403. [PubMed: 23867626]
40. Chen KY, Brychta RJ, Linderman JD, Smith S, Courville A, Dieckmann W, et al. Brown fat activation mediates cold-induced thermogenesis in adult humans in response to a mild decrease in ambient temperature. J Clin Endocrinol Metab. 2013; 98(7):E1218–23. [PubMed: 23780370]
41. Foster DO, Frydman ML. Tissue distribution of cold-induced thermogenesis in conscious warm- or cold-acclimated rats reevaluated from changes in tissue blood flow: the dominant role of brown adipose tissue in the replacement of shivering by nonshivering thermogenesis. Can J Physiol Pharmacol. 1979; 57(3):257–70. [PubMed: 445227]
42. Baba S, Engles JM, Huso DL, Ishimori T, Wahl RL. Comparison of uptake of multiple clinical radiotracers into brown adipose tissue under cold-stimulated and nonstimulated conditions. J Nucl Med. 2007; 48(10):1715–23. [PubMed: 17873137]

43. Nedergaard J, Bengtsson T, Cannon B. Three years with adult human brown adipose tissue. Ann N Y Acad Sci. 2010; 1212:E20–36. [PubMed: 21375707]

44. van Marken Lichtenbelt WD, Vanhommerig JW, Smulders NM, Drossaerts JM, Kemerink GJ, Bouvy ND, et al. Cold-activated brown adipose tissue in healthy men. N Engl J Med. 2009; 360(15):1500–8. [PubMed: 19357405]

45. Ravussin E, Burnand B, Schutz Y, Jequier E. Twenty-four-hour energy expenditure and resting metabolic rate in obese, moderately obese, and control subjects. Am J Clin Nutr. 1982; 35(3):566–73. [PubMed: 6801963]

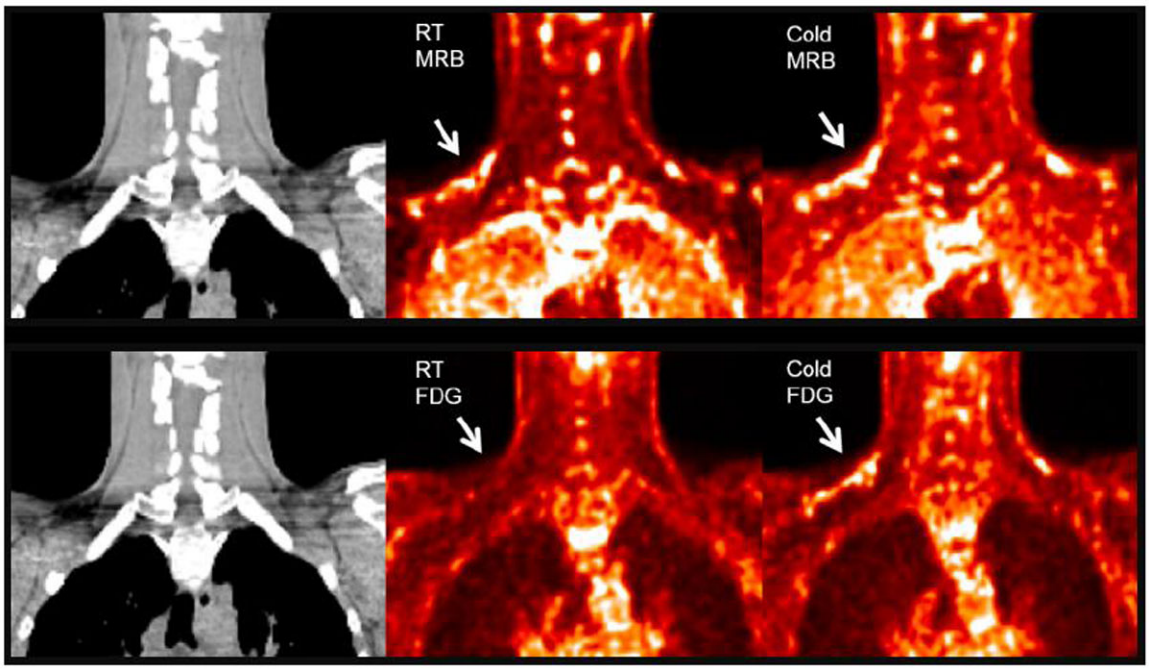

Figure 1.

BAT visualized using RT and cold ^{18}F-FDG compared to RT and cold ^{11}C-MRB in one representative male subject. ^{18}F-FDG and ^{11}C-MRB are scaled from SUV 0 (black) to SUV 2 (white). ^{11}C-MRB images are computed from the average of frames acquired between 40 to 60 min post-injection.

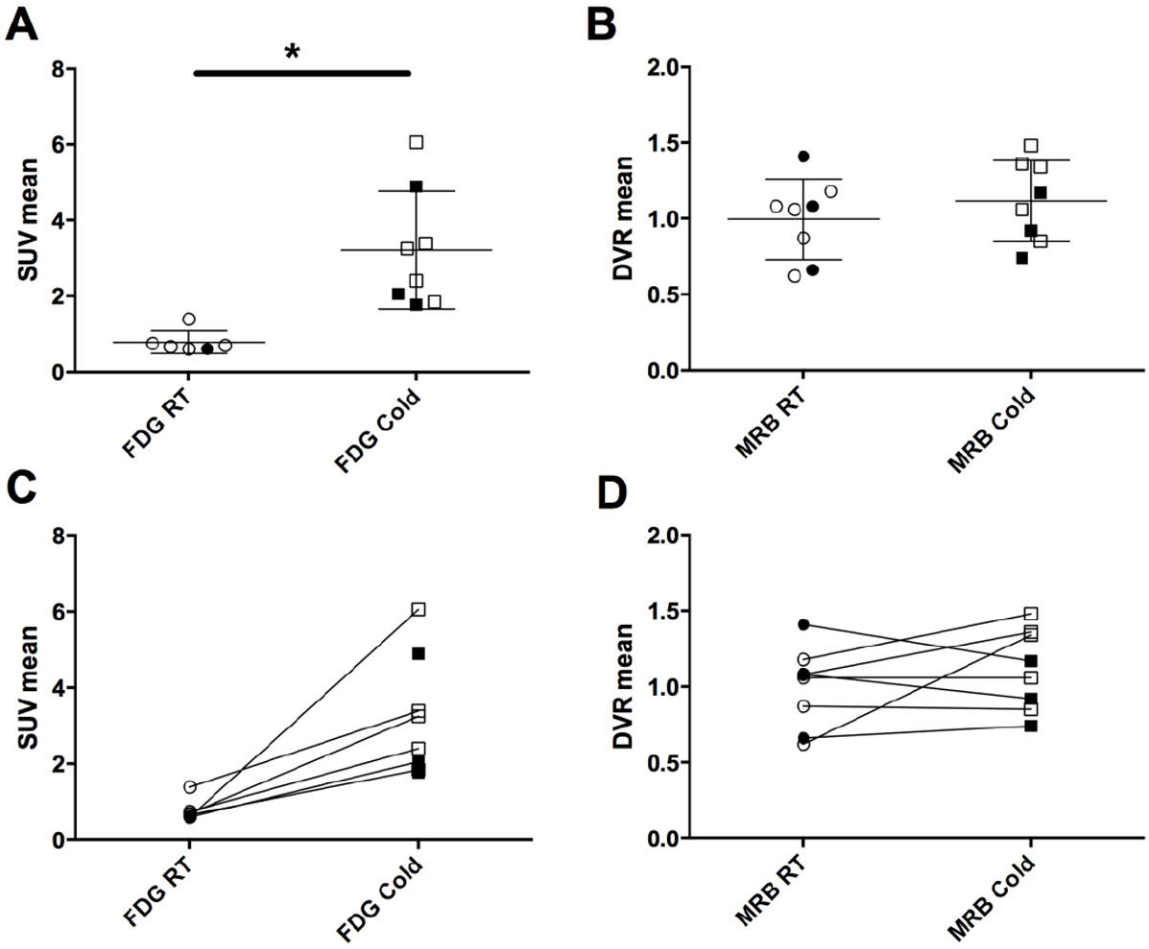

Figure 2.

(A) ^{18}F-FDG and (B) ^{11}C-MRB uptake in supraclavicular BAT under room temperature (RT) and cold stimulated conditions; Change in (C) ^{18}F-FDG and (D) ^{11}C-MRB uptake of individual subjects in supraclavicular BAT between room temperature and cold stimulated conditions. RT FDG scans were not performed for 3 female subjects. * $p<0.05$, open markers = men; closed markers = women

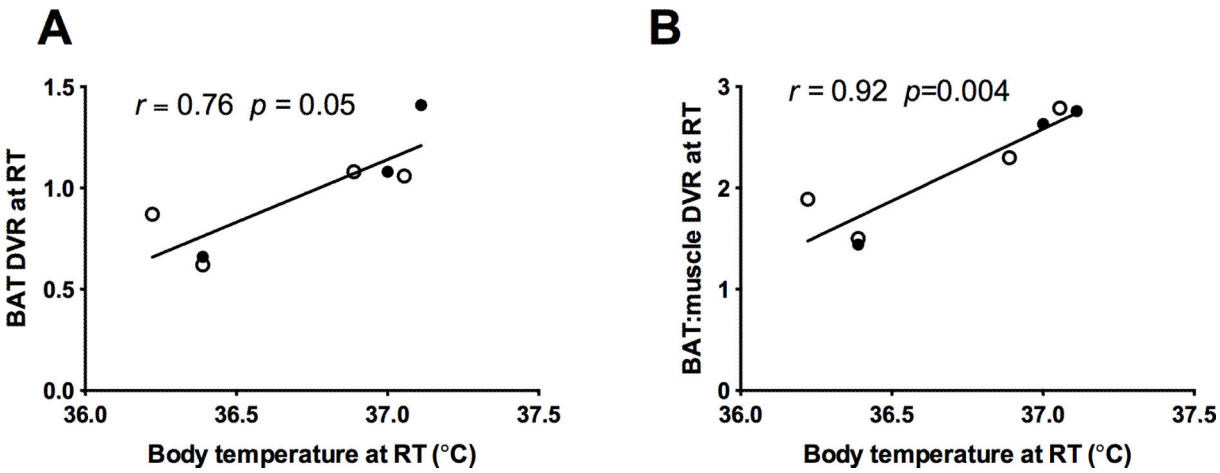

Figure 3.

Relationship between (A) BAT ^{11}C-MRB DVR at RT and (B) BAT:muscle ^{11}C-MRB DVR with body temperature at RT (open circle = men; closed circle = women).

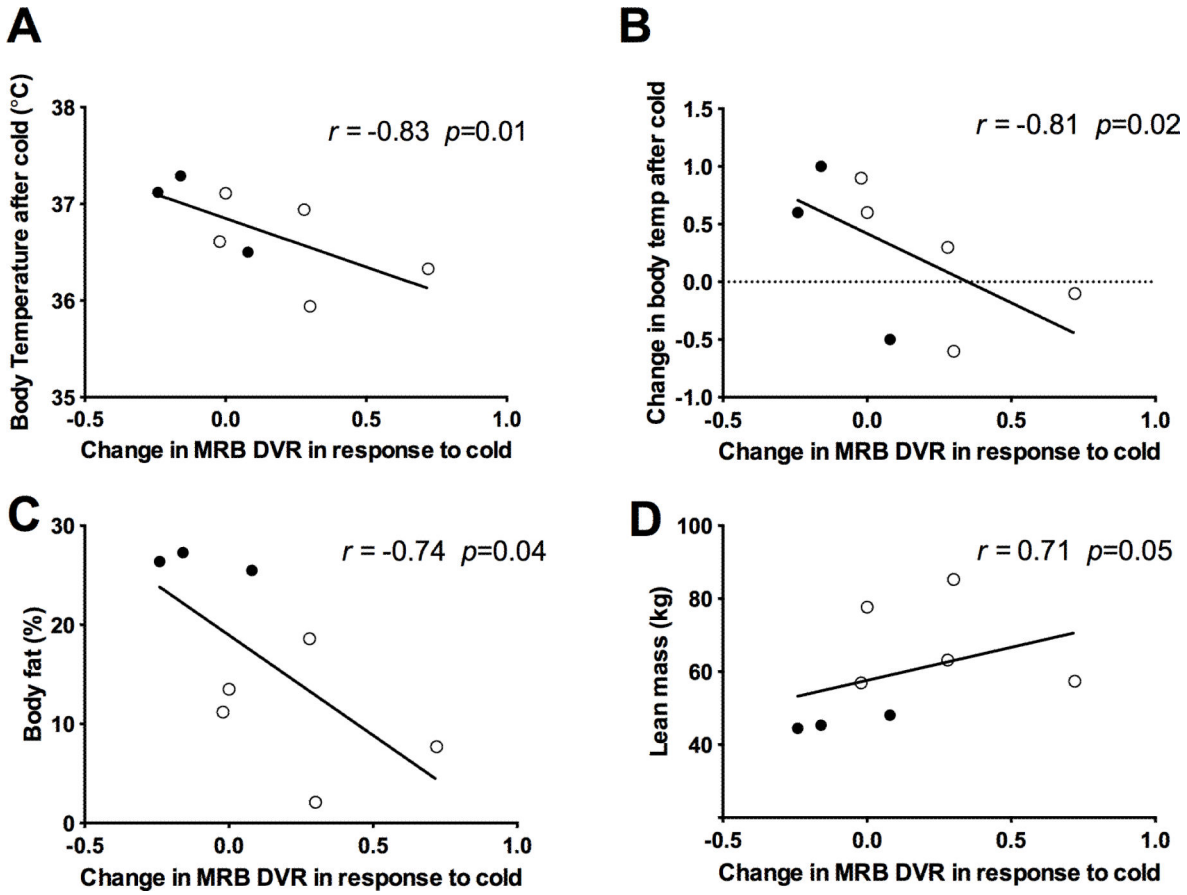

Figure 4.

Relationship between change in MRB uptake in response to cold and (A) body temperature after cold; (B) change in body temperature after cold; (C) percentage body fat; (D) lean body mass (open circle = men; closed circle = women).

Table 1

Characteristics of Study Participants

	Group	Male (n=5)	Female (n=5)	*p*
Age (years)	25.0 ± 2.3	24.6 ± 2.6	25.4 ± 2.1	0.61
BMI (kg/m2)	21.9 ± 2.0	21.6 ± 2.7	22.1 ± 1.0	0.73
Fat mass (kg)	12.1 ± 6.0	8.1 ± 5.2	16.3 ± 3.4	0.02
Body fat (%)	18.7 ± 9.8	10.6 ± 6.2	26.8 ± 3.9	0.001
Lean mass (kg)	56.1 ± 15.4	68.1 ± 12.7	44.0 ± 3.2	0.003
Temp during RT MRB (°C)	36.8 ± 0.1	36.6 ± 0.1	36.9 ± 0.1	0.28
Temp during Cold MRB (°C)	36.8 ± 0.2	36.5 ± 0.1	37.1 ± 0.1	0.09
Resting heart rate (bpm)	67 ± 12	63 ± 9	70 ± 14	0.38
Systolic BP (mm Hg)	109 ± 8	108 ± 5	109 ± 11	0.89
Diastolic BP (mm Hg)	65 ± 5	69 ± 6	62 ± 1	0.05
Mean arterial pressure	77 ± 7	82 ± 6	72 ± 5	0.01

p value for male:female differences